M&C 2017 - International Conference on Mathematics & Computational Methods Applied to Nuclear Science & Engineering, Jeju, Korea, April 16-20, 2017, on USB (2017)

Nonclassical Particle Transport in Heterogeneous Materials

Thomas Camminady[†], Martin Frank[†] and Edward W. Larsen[*]

[†]*Center for Computational Engineering Science, RWTH Aachen University, Schinkelstrasse 2, 52062 Aachen, Germany*
[*]*Department of Nuclear Engineering and Radiological Sciences, University of Michigan, Ann Arbor, MI 48104*
camminady@mathcces.rwth-aachen.de, frank@mathcces.rwth-aachen.de, edlarsen@umich.edu

Abstract - *We present an extension of the pathlength distribution for the nonclassical Boltzmann equation to heterogeneous materials. Since the pathlength distribution $p(s)$ is nonexponential in the nonclassical setting, we propose a potential candidate for the nonclassical heterogeneous pathlength distribution $p(\boldsymbol{x}, \boldsymbol{\Omega}, s)$ that models the particle transport in this setting. The distribution $p(\boldsymbol{x}, \boldsymbol{\Omega}, s)$ is constructed under consideration of the requirements that a generalized pathlength distribution has to fulfill. Motivated by the relation between the nonclassical Boltzmann equation and the SP_N approximations, we perform numerical experiments that compare the angular flux $\phi_0(\boldsymbol{x})$ of several SP_1 computations with the angular flux that a Monte Carlo simulation of the nonclassical Boltzmann equation with the new pathlength distribution yields. For this application, we furthermore present efficient sampling strategies to generate samples from the resulting pathlength distribution.*

I. INTRODUCTION

In recent years, nonclassical particle transport has become a topic of increasing interest [1, 2, 3, 4, 5]. In contrast to the classical theory of Boltzmann, the nonclassical theory describes particle transport where the distance-to-collision is no longer exponentially distributed. In classical particle transport, the distribution for the distance-to-collision is exponential due to the uncorrelated, i. e. Poisson distributed, positioning of scattering centers in the material. However, there exist cases in which the distribution of the distance-to-collision $p(s)$, also referred to as pathlength distribution, is no longer exponential [6, 7, 8]. Whereas particle transport in the classical case is described by the Boltzmann equation that does not depend on the pathlength s, the distance-to-collision does become a dependent variable in the nonclassical case.

In this paper, we consider nonclassical particle transport in heterogeneous materials. Based on the requirements that a generalized distribution for the heterogeneous case has to satisfy, we construct a candidate for the nonclassical heterogeneous pathlength distribution $p(\boldsymbol{x}, \boldsymbol{\Omega}, s)$. We validate that the distribution $p(\boldsymbol{x}, \boldsymbol{\Omega}, s)$ fulfills the posed requirements and is consistent when applying it to the heterogeneous classical setting or the homogeneous nonclassical setting. As generalizing the homogeneous to the heterogeneous case is not unique, we can so far not prove that this is the correct pathlength distribution.

As shown in [9], the nonclassical transport equation with a specific choice of $p(s)$ is capable of reproducing the scalar flux computed via an SP_N calculation. This allows to solve for the scalar flux, obtained by an SP_N computation with any available Monte Carlo method, introducing only statistical errors. We then sample according to $p(\boldsymbol{x}, \boldsymbol{\Omega}, s)$ for heterogeneous computations with a Monte Carlo solver. The resulting scalar flux of the Monte Carlo simulation is then compared with a deterministic reference solver for the SP_N approximations to further validate the candidate.

The outline of this paper is as follows: The theory of nonclassical transport is briefly outlined in Section II. In Section III, we consider the distance-to-collision in presence of interfaces in the classical case. We then propose a generalized expression for the distribution of the distance-to-collision in heterogeneous, nonclassical materials $p(\boldsymbol{x}, \boldsymbol{\Omega}, s)$. This expression is then further analyzed and applied to different heterogeneous materials. Section IV uses the relation between the nonclassical Boltzmann equation and the SP_N approximations and derives a pathlength distribution for the heterogeneous case based on $p(\boldsymbol{x}, \boldsymbol{\Omega}, s)$. Additionally, we propose efficient sampling strategies for these distributions in Section V. Numerical experiments that show agreement between the scalar flux of a Monte Carlo simulation with the proposed pathlength distribution and a reference code for the SP_N approximations are presented in Section VI.

In Section VII, the presented work is concluded with a short discussion and an outline of future work.

II. NONCLASSICAL TRANSPORT

In nonclassical transport, we consider the potential angular collision rate $\psi(\boldsymbol{x}, \boldsymbol{\Omega}, s)$, that is

$$\begin{aligned}\psi(\boldsymbol{x}, \boldsymbol{\Omega}, s) = &\text{ the rate of particles}\\ &\text{positioned at } \boldsymbol{x} \text{ with direction } \boldsymbol{\Omega}\\ &\text{and distance-to-collision } s.\end{aligned} \tag{1}$$

For time-independent, monoenergetic, three-dimensional particle transport with an isotropic source $Q(\boldsymbol{x})$ and isotropic scattering in a homogeneous material, the equation for $\psi(\boldsymbol{x}, \boldsymbol{\Omega}, s)$ is given by

$$\begin{aligned}-\frac{\partial\, \psi(\boldsymbol{x}, \boldsymbol{\Omega}, s)}{\partial s} &+ \boldsymbol{\Omega} \cdot \nabla \psi(\boldsymbol{x}, \boldsymbol{\Omega}, s)\\ &= \frac{p(s)}{4\pi} \int_{4\pi} c\, \psi(\boldsymbol{x}, \boldsymbol{\Omega}', 0)\, d\boldsymbol{\Omega}' + \frac{p(s)}{4\pi} Q(\boldsymbol{x}),\end{aligned} \tag{2}$$

with suitable boundary conditions and c denoting the scattering ratio. Eq. (2) is also referred to, as the "forward" nonclassical Boltzmann equation. When $p(s)$ is nonexponential, also the total cross section Σ_t depends on s, due to the relation [9]

$$\Sigma_t(s) = \frac{p(s)}{1 - \int_0^s p(s')\, ds'}. \tag{3}$$

Note that the pathlength distribution can depend on a material parameter σ via

$$p_\sigma(s) = \sigma p_1(\sigma s). \tag{4}$$

We define $p(s) := p_1(s)$, which can be interpreted as a *base* pathlength distribution, meaning that different distributions can be obtained as a scaled version of the *base* distribution, e.g. when going from e^{-s} to $\sigma e^{-\sigma s}$. Whereas Eq. (2) and Eq. (3) are formulated for the homogeneous case, the pathlength distribution also depends on position $\boldsymbol{x}$ and angle $\boldsymbol{\Omega}$ in a heterogeneous material.

In the following, we assume that even though the material is heterogeneous, it is *structurally similar*, i. e. it is defined by a material parameter $\sigma(\boldsymbol{x})$ and a *base* distribution $p(s)$. The *base* distribution can be used together with Eq. (4) to obtain the distribution for a certain region of the material.

We therefore do not consider materials where the pathlength distribution is classical in some part of the domain and nonclassical in another. Nonetheless, materials with pathlength distribution $\sigma_1 e^{-\sigma_1 s}$ in one region of the domain as well as $\sigma_2 e^{-\sigma_2 s}$ in other regions are admissible since they can both be expressed by the *base* distribution $p(s) = e^{-s}$ and the relation in Eq. (4).

For $p(s) = e^{-s}$ we obtain $\Sigma_t(\boldsymbol{x}) = \sigma(\boldsymbol{x})$, i. e. the material parameter is the classical total cross section. If however, $p(s) = se^{-s}$, then also Σ_t is a function of $s, \boldsymbol{x}$ and $\boldsymbol{\Omega}$, whereas $\sigma(\boldsymbol{x})$ encodes the different materials, meaning we could observe a distribution $p_{\sigma_1}(s) = \sigma_1^2 s e^{-\sigma_1 s}$ in one region of the domain and $p_{\sigma_2}(s) = \sigma_2^2 s e^{-\sigma_2 s}$ in another with cross sections $\Sigma_{t,1}(s) = \sigma_1^2 s/(1+\sigma_1 s)$ and $\Sigma_{t,2}(s) = \sigma_2^2 s/(1+\sigma_2 s)$, respectively.

III. DISTANCE-TO-COLLISION OVER INTERFACES

When considering heterogeneous materials, the question of constructing the distribution of the distance-to-collision over interfaces arises naturally. The situation occurs, when particles located in one material have a direction of flight, such that they pass through one or multiple materials, denoted by $V_1, V_2, ..., V_n$.

For solving the nonclassical transport equation for a concrete realization of the heterogeneous material, we need to construct a distribution for the distance-to-collision $p(\boldsymbol{x}, \boldsymbol{\Omega}, s)$ across the interfaces between different regions of the material. Given a domain V that consists of two materials V_1 and V_2, we start by considering particles positioned at $\boldsymbol{x} \in V_1$ with direction $\boldsymbol{\Omega}$, such that for all $0 \le s \le d(\boldsymbol{x}, \boldsymbol{\Omega})$ we have $\boldsymbol{x} + s\,\boldsymbol{\Omega} \in V_1$ and $\boldsymbol{x} + s\,\boldsymbol{\Omega} \in V_2$ for $s > d(\boldsymbol{x}, \boldsymbol{\Omega})$ as shown in Fig. 1 for a single interface, or in Fig. 2 for the case of multiple interfaces. In the nonclassical heterogeneous case, we use $p(\boldsymbol{x}, \boldsymbol{\Omega}, s)$ as the heterogeneous version of $p(s)$ and interpret it as

$$\begin{aligned} p(\boldsymbol{x}, \boldsymbol{\Omega}, s) = {} & \text{the probability, that a particle at } \boldsymbol{x} \text{ with} \\ & \text{velocity } \boldsymbol{\Omega} \text{ will travel a distance } s \\ & \text{through a (potentially) heterogeneous} \\ & \text{material to collide at } \boldsymbol{x} + s\boldsymbol{\Omega}. \end{aligned} \tag{5}$$

For classical transport, the distribution for the distance-to-collision for heterogeneous materials, consisting of homogeneous subregions, can easily be computed by the relation

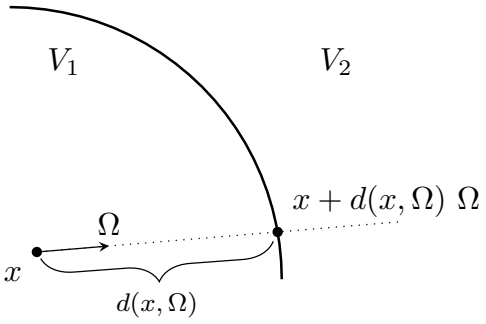

Fig. 1: A particle positioned at $\boldsymbol{x} \in V_1$ with direction $\boldsymbol{\Omega}$ pointing towards material V_2.

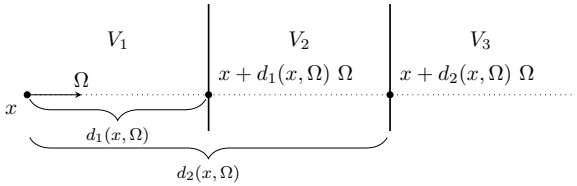

Fig. 2: A particle facing multiple interfaces in the direction of flight.

$$p(\boldsymbol{x}, \boldsymbol{\Omega}, s) = \Sigma_t(\boldsymbol{x} + s\boldsymbol{\Omega}) e^{-\int_0^s \Sigma_t(\boldsymbol{x}+s'\boldsymbol{\Omega})\, ds'}. \tag{6}$$

For the two materials V_1 and V_2 we assume potentially different total cross sections $\Sigma_{t,1}$ and $\Sigma_{t,2}$, such that we can then write Eq. (6) as

$$\begin{aligned} p(\boldsymbol{x}, \boldsymbol{\Omega}, s) = {} & \Sigma_t(\boldsymbol{x} + s\boldsymbol{\Omega}) e^{-\int_0^s \Sigma_t(\boldsymbol{x}+s'\boldsymbol{\Omega})\, ds'} \\ = {} & \begin{cases} \Sigma_{t,1} e^{-\Sigma_{t,1} s}, & s \le d(\boldsymbol{x}, \boldsymbol{\Omega}), \\ \Sigma_{t,2} e^{-\Sigma_{t,1} d(\boldsymbol{x}, \boldsymbol{\Omega}) - \Sigma_{t,2}(s - d(\boldsymbol{x}, \boldsymbol{\Omega}))}, & s > d(\boldsymbol{x}, \boldsymbol{\Omega}). \end{cases} \end{aligned} \tag{7}$$

This result is widely known and standard. However, it is not clear how an appropriate pathlength distribution $p(\boldsymbol{x}, \boldsymbol{\Omega}, s)$ might look like in presence of one or multiple interfaces, given a nonclassical heterogeneous material.

While generalizing the distribution for nonclassical materials is not unique, there are requirements that potential candidates must satisfy.

I. Since we are interested in probability density functions, we require

$$\int_0^\infty p(\boldsymbol{x}, \boldsymbol{\Omega}, s')\, ds' = 1, \tag{8}$$

independent the composition of the different materials, $\boldsymbol{x}$ or $\boldsymbol{\Omega}$.

II. For an exponential pathlength distribution in the different materials we want to recover Eq. (6).

III. In the case where the material is completely homogeneous, i. e. $\sigma(\boldsymbol{x}) = \sigma$, the heterogeneous distribution $p(\boldsymbol{x}, \boldsymbol{\Omega}, s)$ has to reduce to the classical or nonclassical, homogeneous distribution $p(s)$.

IV. Assume that a particle experiences its next collision before crossing an interface. The distribution of pathlengths under this assumption should match the pathlength distribution of the material the particle is positioned in.

V. While $p(\boldsymbol{x}, \boldsymbol{\Omega}, s)$ is not necessarily continuous over an interface, $p(\boldsymbol{x}, \boldsymbol{\Omega}, s)/\sigma(\boldsymbol{x} + s\boldsymbol{\Omega})$ has to be continuous.

We will now propose a potential candidate for the nonclassical pathlength distribution $p(\boldsymbol{x}, \boldsymbol{\Omega}, s)$ in a heterogeneous (but *structurally similar*) material, defined by the material parameter $\sigma(\boldsymbol{x})$ and the *base* distribution $p(s)$, and validate that all posed requirements are satisfied. This candidate is given by

$$p(\boldsymbol{x}, \boldsymbol{\Omega}, s) := \sigma(\boldsymbol{x} + s\boldsymbol{\Omega})\, p\left(\int_0^s \sigma(\boldsymbol{x} + s'\boldsymbol{\Omega})\, ds'\right) \tag{9a}$$

$$= p_{\sigma(\boldsymbol{x}+s\boldsymbol{\Omega})}\left(\int_0^s \frac{\sigma(\boldsymbol{x} + s'\boldsymbol{\Omega})}{\sigma(\boldsymbol{x} + s\boldsymbol{\Omega})}\, ds'\right), \tag{9b}$$

where the equality holds due to the scaling property introduced by Eq. (4). The cumulative distribution function is then given by

$$\begin{aligned} P(\boldsymbol{x}, \boldsymbol{\Omega}, s) &= \int_0^s p(\boldsymbol{x}, \boldsymbol{\Omega}, s')\, ds' \\ &= P\left(\int_0^s \sigma(\boldsymbol{x} + s'\boldsymbol{\Omega})\, ds'\right), \end{aligned} \tag{10}$$

where $P(\cdot)$ denotes the cumulative distribution function of the *base* density. Therefore, $P(\boldsymbol{x}, \boldsymbol{\Omega}, s)$ is a valid cumulative distribution function and requirement I is satisfied. Assume now that $p(s) = e^{-s}$. By definition

$$p(\boldsymbol{x}, \boldsymbol{\Omega}, s) = \sigma(\boldsymbol{x} + s\boldsymbol{\Omega})\, e^{-\int_0^s \sigma(\boldsymbol{x}+s'\boldsymbol{\Omega})\, ds'}, \tag{11}$$

which is the correct reduction to the classical case, thus fulfilling requirement II as well, since $\sigma = \Sigma_t$ holds in this case. For a homogeneous material $\sigma(\boldsymbol{x})$ is constant, e. g. $\sigma(\boldsymbol{x}) = \sigma$. Then Eq. (9a) correctly satisfies requirement III by

$$p(\boldsymbol{x}, \boldsymbol{\Omega}, s) = \sigma p(\sigma s) = p_\sigma(s). \tag{12}$$

Requirement IV is also satisfied since $p(\boldsymbol{x}, \boldsymbol{\Omega}, s)$ is only influenced by the material that is at most a distance s away from position $\boldsymbol{x}$. Finally, it is easy to see that $p(\boldsymbol{x}, \boldsymbol{\Omega}, s)/\sigma(\boldsymbol{x} + s\boldsymbol{\Omega})$ is continuous.

IV. RELATION WITH THE SP$_N$ APPROXIMATIONS

The simplified P$_N$ equations are leading and high order approximations of the transport equation [10, 11]. As an example of the SP$_N$ approximations, the SP$_1$ approximation is given by

$$-\nabla \cdot \frac{1}{3\sigma(\boldsymbol{x})} \nabla \Phi_0(\boldsymbol{x}) + \sigma(\boldsymbol{x})\Phi_0(\boldsymbol{x}) = c\sigma(\boldsymbol{x})\Phi_0(\boldsymbol{x}) + Q(\boldsymbol{x}). \tag{13}$$

Here, $\Phi_0(\boldsymbol{x})$ denotes the scalar flux, $Q(\boldsymbol{x})$ the isotropic source, $\sigma(\boldsymbol{x})$ the total cross section and c the scattering ratio. (*Note:* We use $\sigma(\boldsymbol{x})$ as the total cross section and not $\Sigma_t(\boldsymbol{x})$. This is done to avoid confusion when we later derive an expression for a corresponding nonclassical pathlength distribution $p(\boldsymbol{x}, \boldsymbol{\Omega}, s)$ and the nonclassical total cross section $\Sigma(\boldsymbol{x}, \boldsymbol{\Omega}, s)$ in terms of $\sigma(\boldsymbol{x})$. However, $\sigma(\boldsymbol{x})$ is exactly the material parameter that corresponds to the total cross section in the context of the diffusion approximations.)

Even though the SP$_1$ approximation is exactly the P$_1$ approximation, we will refer to it as SP$_1$ to emphasize that we are in the context of the SP$_N$ approximations. It has recently been shown [9] that the SP$_1$, SP$_2$ and SP$_3$ equations, can be represented by the so-called "backward" nonclassical transport equation with only statistical errors when $p(s)$ is chosen appropriately. Whereas Eq. (2) is referred to as the "forward" nonclassical transport equation, as s describes the distance-to-collision, the s variable is interpreted as the distance-since-collision in the "backward" nonclassical transport equation. However, equivalence between the two equations has been shown in the case of an unbounded domain [12], but can also be derived for bounded domains with suitable initial conditions [13]. With $f(\boldsymbol{x}, \boldsymbol{\Omega}, s)$ as the solution of the "backward" equation and $\psi(\boldsymbol{x}, \boldsymbol{\Omega}, s)$ as the solution of the "forward" equation, we obtain the relation

$$\psi(\boldsymbol{x}, \boldsymbol{\Omega}, 0) = \int_0^\infty \Sigma_t(s') f(\boldsymbol{x}, \boldsymbol{\Omega}, s')\, ds', \tag{14}$$

for an unbounded domain. Integrating out the angular dependency yields

$$\begin{aligned} \int_{4\pi} \psi(\boldsymbol{x}, \boldsymbol{\Omega}', 0)\, d\boldsymbol{\Omega}' &= \int_{4\pi} \int_0^\infty \Sigma_t(s') f(\boldsymbol{x}, \boldsymbol{\Omega}', s')\, ds' d\boldsymbol{\Omega}' \\ &= r(\boldsymbol{x}), \end{aligned} \tag{15}$$

where the right-hand side denotes the collision rate density. The collision rate density and the scalar flux $\phi(\boldsymbol{x})$ are related by $r(\boldsymbol{x}) = \sigma(\boldsymbol{x})\phi_0(\boldsymbol{x})$, which allows the computation of the scalar flux by

$$\phi_0(\boldsymbol{x}) = \frac{1}{\sigma(\boldsymbol{x})} \int_{4\pi} \psi(\boldsymbol{x}, \boldsymbol{\Omega}', 0)\, d\boldsymbol{\Omega}', \tag{16}$$

for $\sigma(\boldsymbol{x}) > 0$. Since $\psi(\boldsymbol{x}, \boldsymbol{\Omega}, 0)$ is the result, computed by a Monte Carlo simulation, we obtain an immediate way to deduce the scalar flux. With the right choice of $p(s)$, this scalar flux then matches the scalar flux that an SP$_1$ computation

would yield. The corresponding pathlength distribution for a homogeneous material, i. e. $\sigma(\boldsymbol{x}) = \sigma$, reads

$$p_{\sqrt{3}\sigma}(s) = 3\sigma^2 s e^{-\sqrt{3}\sigma s}. \tag{17}$$

This matches the probability density function of the Gamma distribution, given by

$$\gamma(s, k, \theta) = \frac{1}{\Gamma(k)\theta^k} s^{k-1} e^{-x/\theta}, \tag{18}$$

for the case $k = 2$ and $\theta^{-1} = \sqrt{3}\sigma$. In the case of a heterogeneous material, we can use Eq. (9a) to obtain the new probability density function. Our *base* distribution for the SP_1 approximation is therefore given by

$$p(s) = s e^{-s}, \tag{19}$$

since

$$\begin{aligned} p_{\sqrt{3}\sigma}(s) &= 3\sigma^2 s e^{-\sqrt{3}\sigma s} \\ &= \sqrt{3}\sigma p(\sqrt{3}\sigma s). \end{aligned} \tag{20}$$

For simplicity let us again consider the setting described by Fig. 1. A particle is positioned at $\boldsymbol{x} \in V_1$ with velocity $\boldsymbol{\Omega}$ and will cross the interface to region V_2 after traveling a distance $d = d(\boldsymbol{x}, \boldsymbol{\Omega})$. We then write the heterogeneous pathlength distribution in this context as

$$\begin{aligned} p(s, d) = {} & \text{the probability that a particle positioned} \\ & \text{in } V_1 \text{ will travel distance } s \\ & \text{with the interface between } V_1 \text{ and } V_2 \\ & \text{positioned a distance } d \text{ away.} \end{aligned} \tag{21}$$

By using the proposed distribution from Eq. (9a), we obtain for $\sigma(s) = \sigma_1/\sqrt{3}$ if $s \le d$ and $\sigma(s) = \sigma_2/\sqrt{3}$ if $s > d$ the heterogeneous pathlength distribution for the SP_1 approximation in the setting introduced by Fig. 1 as

$$\begin{aligned} p(s, d) &= \begin{cases} p_{\sigma_1}(s), & s \le d, \\ p_{\sigma_2}\left(\dfrac{\sigma_1 d + \sigma_2(s-d)}{\sigma_2}\right), & s > d \end{cases} \\ &= \begin{cases} \sigma_1 p(\sigma_1 s), & s \le d, \\ \sigma_2 p\left(\sigma_1 d + \sigma_2(s-d)\right), & s > d \end{cases} \\ &= \begin{cases} \sigma_1^2 s e^{-\sigma_1 s}, & s \le d, \\ \dfrac{e^{-\sigma_1 d}}{e^{-\sigma_2 d}} \sigma_2 \left((\sigma_1 - \sigma_2)d + \sigma_2 s\right) e^{-\sigma_2 s}, & s > d. \end{cases} \end{aligned} \tag{22}$$

As before, $p(s, d)$ depends on $\boldsymbol{x}$ and $\boldsymbol{\Omega}$ by $d = d(\boldsymbol{x}, \boldsymbol{\Omega})$. An example of the distributions defined by Eq. (22) and the corresponding cumulative distribution is given in Fig. 3. We observe, that $p(s, d)$ might potentially be discontinuous, while $p(s, d)/\sigma(s)$ is always continuous. The result again generalizes for the case of multiple interfaces and also for $\sigma(\boldsymbol{x})$ which are not piecewise constant as illustrated in Fig. 4 where we see the different pathlength distributions for a material parameter

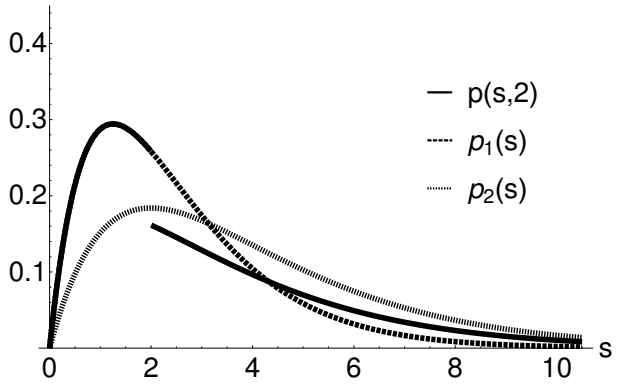

(a) Probability density function

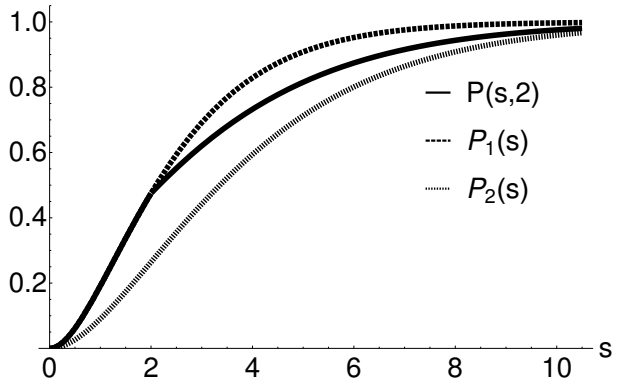

(b) Cumulative distribution function

Fig. 3: (a) The probability density functions for the distance-to-collision with $\sigma_1 = 0.8$, $\sigma_2 = 0.5$ and $d = 2$. (b) The corresponding cumulative distribution functions.

$\sigma(\boldsymbol{x})$. We again observe the continuity of $p(\boldsymbol{x}, \boldsymbol{\Omega}, s)/\sigma(\boldsymbol{x} + s\boldsymbol{\Omega})$. Fig. 4 assumes the *base* distribution to be nonclassical and of the form $p(s) = s e^{-s}$ throughout (a), (b) and (c).

For the higher order approximations, the corresponding *base* pathlength distributions in the homogeneous setting are given by

$$p(s) = \frac{5}{9}\delta(s) + \frac{4}{9} s e^{-s} \tag{23}$$

for the SP_2 approximation and

$$p(s) = s\left(A^+ e^{-\lambda^+ s} + A^- e^{-\lambda^- s}\right) \tag{24}$$

for the SP_3 approximation, respectively, where A^+, A^-, λ^+ and λ^- are given in [9]. The presence of $\delta(s)$ in the SP_2 distributions corresponds to an immediate collision without traveling any further distance. The distribution functions are presented in Fig. 5 together with the classical exponential pathlength distribution.

V. SAMPLING STRATEGIES

For the case of nonexponential distributions, the sampling procedure becomes more difficult. Even though inside a material, the distance-to-collision for the SP_1 approximation is Gamma distributed and a superposition of two Gamma

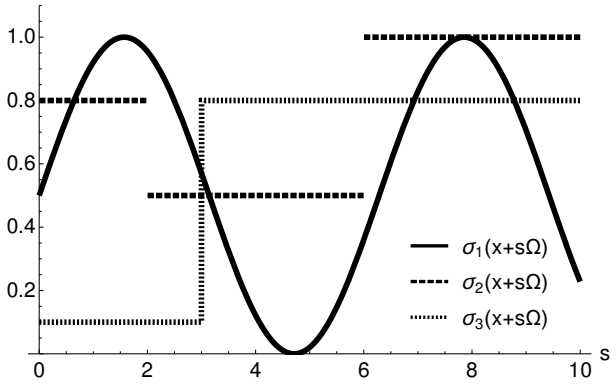

(a) Material parameter $\sigma(\boldsymbol{x} + s\boldsymbol{\Omega})$

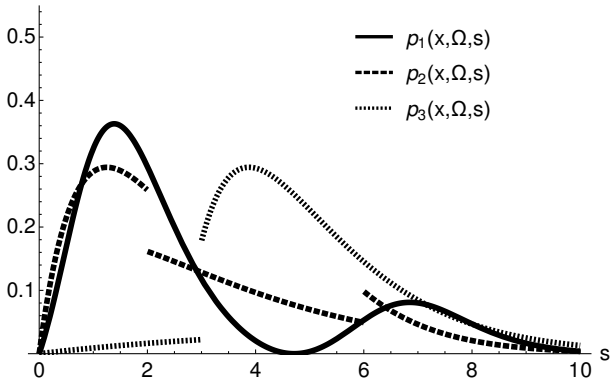

(b) Pathlength distribution for the different materials

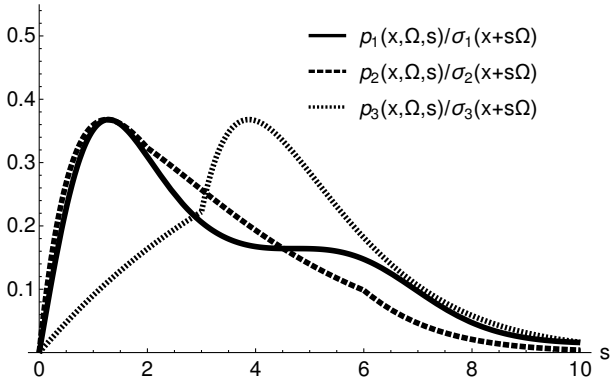

(c) Continuity of $p(\boldsymbol{x}, \boldsymbol{\Omega}, s)/\sigma(\boldsymbol{x} + s\boldsymbol{\Omega})$

Fig. 4: (a) Different materials defined by the material parameter $\sigma(\boldsymbol{x} + s\boldsymbol{\Omega})$. (b) The corresponding pathlength distributions. (c) The ratio of pathlength distribution and material parameter is continuous.

distributions for the SP_3 approximation, sampling from the constructed distribution over an interface is nontrivial. Since the cumulative distribution function can be computed analytically, we can always use inverse sampling to generate samples from the required pathlength distributions. Given a cumulative density function $P(s, d_1, ..., d_n)$ for a particle facing n interfaces at distances $d_1, ..., d_n$ away in the direction of flight, we can use Newton's method to solve $P(s, d_1, ..., d_n) - u = 0$ with $u \sim \mathcal{U}[0, 1]$. To accelerate the procedure, the branch

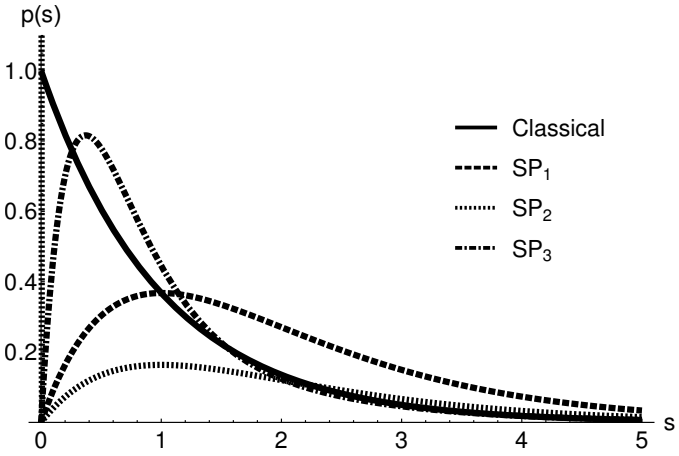

Fig. 5: Pathlength distribution in the classical case and for the SP_N approximations.

of the cumulative distribution function is selected at first by computing i, such that $P(d_{i-1}, d_1, ..., d_n) < u \leq P(d_i, d_1, ..., d_n)$. We then apply Newton's method to compute the exact distance a particle will move. An additional acceleration has been observed, when applying Newton's method to the problem $\log(P(s, d_1, ..., d_n)) - \log(u) = 0$ instead of the original problem. Note, that this procedure is mostly independent of the number of interfaces a particle is facing, as only the selection of the correct branch depends on the material composition.

Consider now again the setting of Fig. 1 with $\sigma(s) = \sigma_1$ for $s \leq d$ and $\sigma(s) = \sigma_2$ otherwise. Given particles at $\boldsymbol{x}$ with direction $\boldsymbol{\Omega}$ facing only one interface in the direction of flight, we propose Algorithm 1 to generate samples for the SP_1 approximation for which samples are distributed according to Eq. (22), Algorithm 2 for the SP_2 case and Algorithm 3 for the SP_3 approximation, respectively.

By substituting $s = s' + d$ in Eq. (22), the case for $s > d$ can be rewritten as

$$\begin{aligned} p(s') =& \alpha 3\sigma_2^2 s' e^{-\sqrt{3}\sigma_2 s'} \\ &+ (1-\alpha)\,\sigma_2 e^{-\sqrt{3}\sigma_2 s'}, \end{aligned} \tag{25}$$

with $\alpha^{-1} = 1 + d\sqrt{3}\sigma_1$. This means that s' is sampled from a Gamma distribution with probability α and from an exponential distribution with probability $(1 - \alpha)$. Therefore, to generate samples for the SP_1 approximation, we sample s from $\gamma\left(2, 1/\left(\sqrt{3}\sigma_1\right)\right)$, i. e. Gamma distributed with parameter $k = 2$ and $\theta^{-1} = \sqrt{3}\sigma_1$. If $s \leq d$ we accept this sample. Otherwise, sample $\alpha \sim \mathcal{U}[0, 1]$. If $\alpha \leq 1/(1+d\sqrt{3}\sigma_1)$ we sample s' from a Gamma distribution with $k = 2$ and $\theta^{-1} = \sqrt{3}\sigma_2$ and return $s' + d$. However, for the case $\alpha > 1/(1 + d\sqrt{3}\sigma_1)$, we sample s' from an exponential distribution $\mathcal{E}xp(\sqrt{3}\sigma_2)$ and return $s' + d$. This procedure is summarized in the first Algorithm on the next page.

To sample from the corresponding SP_2 distribution, we can modify Algorithm 1 to return a step of length 0 with probability 5/9 and to sample from the original algorithm with probability 4/9 otherwise, presented in Algorithm 2.

Algorithm 1 SP_1 Sampling

procedure SAMPLESP$_1(d, \sigma_1, \sigma_2)$
  Sample $s \sim \gamma\left(2, 1/\left(\sqrt{3}\sigma_1\right)\right)$
  if $s < d$ **then**
    return s
  else
    Sample $\alpha \sim \mathcal{U}[0, 1]$
    if $\alpha < 1/\left(1 + d\ \sqrt{3}\sigma_1\right)$ **then**
      Sample $s' \sim \gamma\left(2, 1/\left(\sqrt{3}\sigma_2\right)\right)$
      return $s' + d$
    else
      Sample $s' \sim \mathcal{E}xp(\sqrt{3}\sigma_2)$
      return $s' + d$
    end if
  end if
end procedure

Algorithm 2 SP_2 Sampling

procedure SAMPLESP$_2(d, \sigma_1, \sigma_2)$
  Sample $\alpha \sim \mathcal{U}[0, 1]$
  if $\alpha < 5/9$ **then**
    return 0
  else
    return SampleSP$_1(d, \sigma_1, \sigma_2)$
  end if
end procedure

Algorithm 3 SP_3 Sampling

procedure SAMPLESP$_3(d, \sigma_1, \sigma_2)$
  Sample $\alpha \sim \mathcal{U}[0, 1]$
  if $\alpha < A^+/(A^+ + A^-)$ **then**
    return SampleSP$_1(d, \lambda^+\sigma_1, \lambda^+\sigma_2)$
  else
    return SampleSP$_1(d, \lambda^-\sigma_1, \lambda^-\sigma_2)$
  end if
end procedure

Since the pathlength distribution for the SP_3 distribution $p(s) = s\left(A^+e^{-\lambda^+ s} + A^-e^{-\lambda^- s}\right)$ is a superposition of Gamma distributions we can reuse Algorithm 1 to sample the pathlength. Therefore, we only need to sample a uniform random number to determine which of the Gamma distributions to select and then sample according to Algorithm 1 as shown in Algorithm 3.

Sampling from Algorithm 1 requires one uniform sample and two Gamma samples in the worst case and one Gamma sample in the best case, respectively. For the SP_2 and SP_3 sampling we require one more uniform sample. The output of Algorithm 1, 2 and 3 agree with the corresponding probability density function, shown in Fig. 6 for Algorithm 1 and 3.

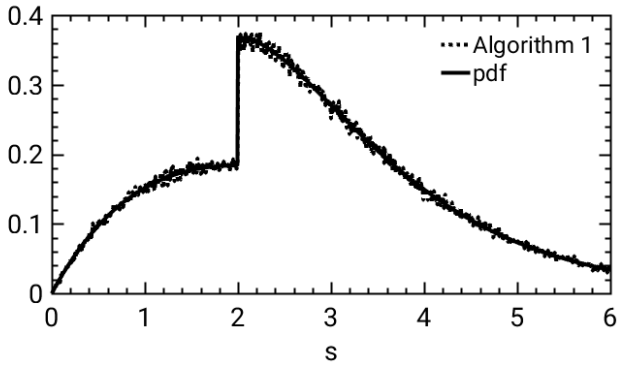

(a) Sampling according to Algorithm 1 compared with the probability density function.

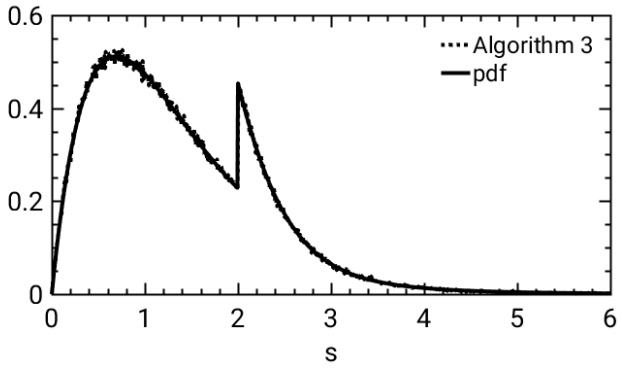

(b) Sampling according to Algorithm 3 compared with the probability density function

Fig. 6: The sampling output from Algorithm 1 and Algorithm 2 compared wit the probability density function for the setting of a single interface distance d away with $\sigma_1 = 0.5, \sigma_2 = 1$ and $d = 2$.

VI. NUMERICAL EXPERIMENTS

Additionally to an efficient sampling strategy, we also need a fast grid traversing algorithm, that can compute the distance to the different interfaces that a particle might pass through. However, for cartesian geometries these distances can be computed efficiently by standard algorithms. In the following, we therefore assume that these distances are available inside a Monte Carlo code.

In our first numerical experiment, we consider the SP_1 equation in one dimension for which we can compute the analytic solution for the heterogeneous material. We compare this analytic solution with the scalar flux of a pseudo 3D Monte Carlo simulation, using the pathlength distribution of Eq. (22). Even though we sample the direction Ω from $\mathbb{S}^2$, we ignore the y and z component and move particles only in x direction. (*Note:* This is different from simulation in rod geometry where we would choose $\Omega \in \{-1, 1\}$.) The particles are emitted at $x = -0.1$ and the infinite, purely absorbing material is defined by $\sigma(x) = \sigma_1$ for $x < 0$ and $\sigma(x) = \sigma_2$ in the case $x \geq 0$. The scalar flux $\phi(x)$ agrees with the analytic solution as shown in Fig. 7 and the numerical solution converges against

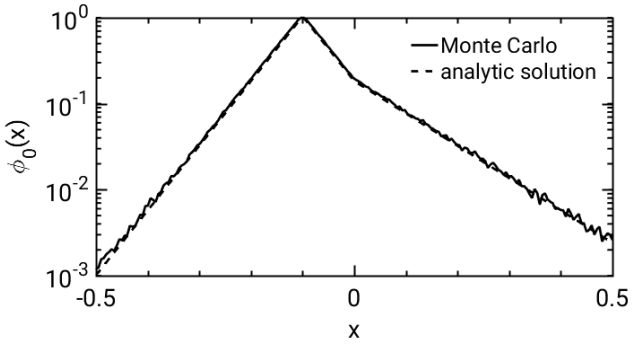

(a) Computation of the 1D scalar flux $\phi_0(x)$ for the Monte Carlo solver against the analytic solution with $\sigma_1 = 10$ and $\sigma_2 = 5$.

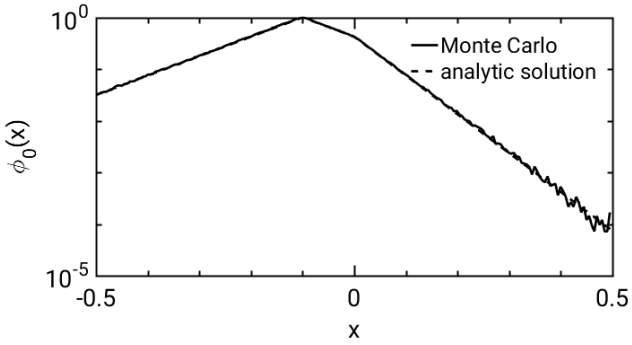

(b) Computation of the 1D scalar flux $\phi_0(x)$ for the Monte Carlo solver against the analytic solution with $\sigma_1 = 5$ and $\sigma_2 = 10$.

Fig. 7: Using the 3D Monte Carlo solver to produce the scalar flux of the 1D version of the SP_1 equation for the single interface problem with two different material compositions in (a) and (b).

the analytic solution with the expected order $N^{1/2}$ where N denotes the number of particles.

We now consider two further test cases. In both cases, the solution of a deterministic SP_1 solver is compared with the computation of a Monte Carlo solver that samples the path-length of every particle from the corresponding distribution. For simplicity, we restrict ourselves to a single interface problem. Let $\boldsymbol{x} = (x, y, z)^T \in \mathbb{R}^3$ and $\boldsymbol{\Omega} \in \mathbb{S}^2$, $\sigma(\boldsymbol{x}) = \sigma(y) = \sigma_{Up}$ for $y \geq 0$ and $\sigma(\boldsymbol{x}) = \sigma(y) = \sigma_{Down}$ for $y < 0$. The setting is again pseudo 3D, meaning that we do sample Ω from $\mathbb{S}^2$, but only move particles in the x and y position and ignore the z component. A source with radius r emits particles isotropically. In both cases we sample $N = 10^6$ particles and compute $\phi_0(\boldsymbol{x})$ on a grid with resolution $N_x = N_y = 200$. For both, the deterministic and the Monte Carlo simulation, we assume a purely absorbing, infinite material without scattering. For $\sigma_{Up} = 1, \sigma_{Down} = 5$ and a source with position $(x, y) = (0, 0.1)$ and radius 0.01 the value of $\log(\phi_0(\boldsymbol{x}))$ for the Monte Carlo simulation and for the deterministic one can be seen in Fig. 8. In the second example, we use $\sigma_{Up} = 2, \sigma_{Down} = 3$ and a source with radius 0.1 positioned at $(x, y) = (0, 0)$. Again, the results for $\log(\phi_0(\boldsymbol{x}))$ are presented for the Monte Carlo simulation and for the deterministic solver in Fig. 9.

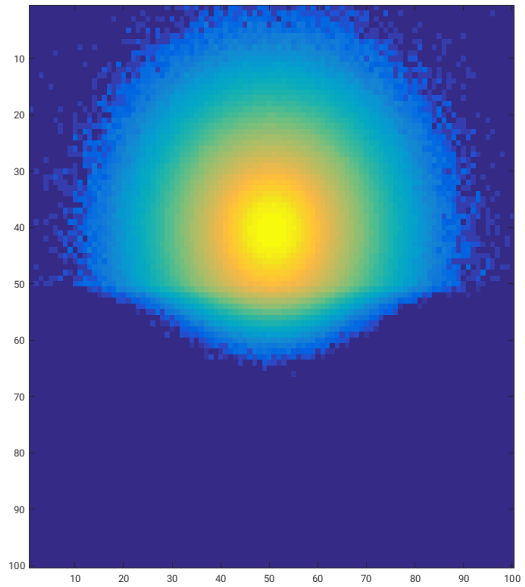

(a) $\log(\phi_0(\boldsymbol{x}))$ for the Monte Carlo solver.

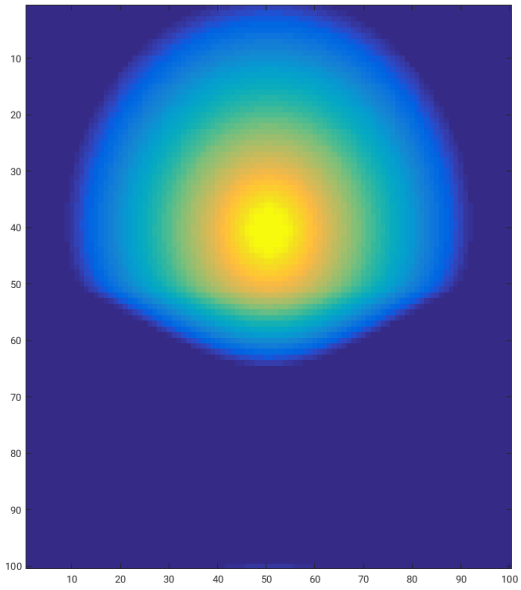

(b) $\log(\phi_0(\boldsymbol{x}))$ for the reference solver.

Fig. 8: The results of a Monte Carlo simulation for the SP_1 equation vs. a deterministic solver. $\sigma_{Up} = 1$ and $\sigma_{Down} = 5$. The color coding is according to $\log(\phi_0(\boldsymbol{x}))$.

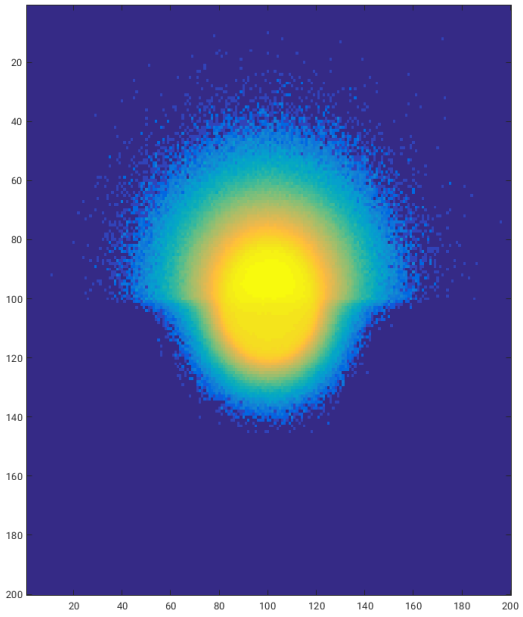

(a) $\log(\phi_0(\boldsymbol{x}))$ for the Monte Carlo solver.

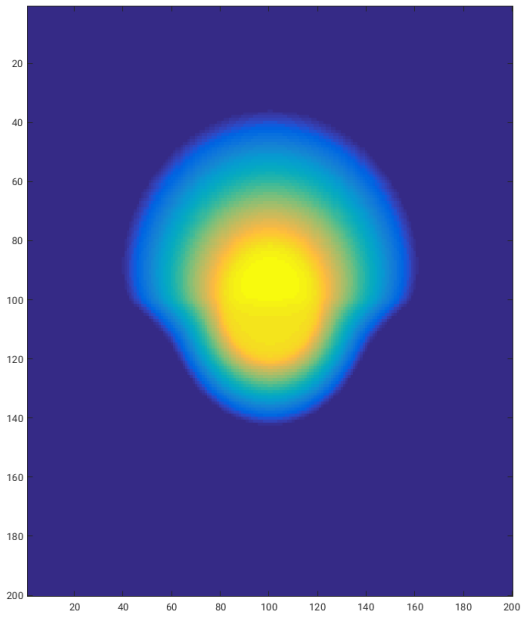

(b) $\log(\phi_0(\boldsymbol{x}))$ for the reference solver.

Fig. 9: The results of a Monte Carlo simulation for the SP_1 equation vs. a deterministic solver. $\sigma_{Up} = 2$ and $\sigma_{Down} = 3$. The color coding is according to $\log(\phi_0(\boldsymbol{x}))$.

While these are first numerical results, they indicate good agreement of the deterministic SP_1 solution and the SP_1 solution obtained by a Monte Carlo simulation of the nonclassical Boltzmann equation with the corresponding pathlength distribution. Note, that in all simulations, $\phi_0(\boldsymbol{x})$ is continuous over the interface for the deterministic and the Monte Carlo solution. The agreement, indicates that the generalized pathlength distribution reduces to the correct expression for the SP_1 approximation under the assumption of a material with piecewise constant $\sigma(\boldsymbol{x})$.

VII. DISCUSSION

We have analyzed nonclassical particle transport in heterogeneous materials. As particle transport is determined by the pathlength distribution, the existing formulations have to be extended to the heterogeneous case. A heterogeneous nonclassical pathlength distribution has to fulfill certain requirements that are discussed. Based on these requirements, we have constructed a possible pathlength distribution $p(\boldsymbol{x}, \boldsymbol{\Omega}, s)$ for the heterogeneous case. As the nonclassical Boltzmann equation is related to the SP_N approximations, we want to use this relation to numerically validate the generalized pathlength distribution since we can not prove it to be correct analytically. For the resulting sampling strategies, we provide efficient algorithms in the general case (i. e. inverse sampling) and Algorithm 1, 2 and 3 for the single interface situation, which can also be extended to multiple interfaces (even though the cost will increase in this case). The numerical experiments indicate that the heterogeneous pathlength distribution is valid for the SP_1 case as the scalar flux $\phi_0(\boldsymbol{x})$ of a Monte Carlo simulation is in good agreement with a deterministic reference solution. While these results suggest that the expression for the heterogeneous pathlength distribution $p(\boldsymbol{x}, \boldsymbol{\Omega}, s)$ is correct, more complex simulations have to be investigated in further numerical experiments.

Furthermore, it remains to validate the proposed pathlength distribution apart from the context of the SP_N approximation in a general setting.

VIII. ACKNOWLEDGMENTS

The authors thank Hossein Gorji for his contribution on the sampling strategy for the SP_1 pathlength distribution.

REFERENCES

1. E.W. Larsen, "A Generalized Boltzmann Equation for 'Non-Classical' Particle Transport," *Proc. Joint International Topical Meeting on Mathematics & Computations and Supercomputing in Nuclear Applications, M&C+SNA 2007*, April 15-19, 2007, Monterey, California (2007).
2. M. Frank and T. Goudon, "On a Generalized Boltzmann Equation for Non-Classical Particle Transport," *Kinetic & Related Models,* **3**, 395 (2010).
3. J. Marklof, and A. Strömbergsson, "Generalized linear Boltzmann equations for particle transport in polycrystals,"*Applied Mathematics Research eXpress* (2015).

4. F. Golse, "Recent results on the periodic Lorentz gas," *Nonlinear Partial Differential Equations,* (2012).
5. R. Vasques and E.W. Larsen, "Non-Classical Particle Transport with Angular-Dependent Path-Length Distributions. I: Theory," *Ann. Nucl. Energy,* Vol. 70, pp. 292-300 (2014).
6. J. Marklof and A. Strömbergsson, "The Distribution of Free Path Lengths in the Periodic Lorentz Gas and Related Lattice Point Problems," *Ann. Math.* Vol. 172, pp. 1949-2033 (2010).
7. J. Marklof and A. Strömbergsson, "Power-Law Distributions for the Free Path Length in Lorentz Gases," *J. Stat. Phys.* Vol. 155, pp. 1072-1086 (2014).
8. R. Vasques and K. Krycki , "On the Accuracy of the Non-Classical Transport Equation in 1-D Random Periodic Media," *arXiv* preprint arXiv:1412.3386 (2014).
9. M. Frank, K. Krycki, E.W. Larsen, and R. Vasques, "The Non-Classical Boltzmann Equation, and Diffusion-Based Approximations to the Boltzmann Equation," *SIAM J. Appl. Math*, Vol. 75, p. 1329 (2015).
10. E.W. Larsen, J. E. Morel, J. M. McGhee. "Asymptotic derivation of the simplified P N equations," *Proc. Joint International Topical Meeting on Mathematics & Computations and Supercomputing in Nuclear Applications, M&C+SNA 1993*, Karlsruhe, Germany (1993).
11. Pomraning, G. C. "Asymptotic and variational derivations of the simplified PN equations." Annals of Nuclear Energy 20.9 (1993): 623-637.
12. K. Krycki, "Mathematical Modeling and Numerical Methods for Non-classical Transport in Correlated Media," Ph.D. Thesis, RWTH Aachen University (2015).
13. E. W. Larsen, M. Frank and T. Camminady "The Equivalence of 'Forward' and 'Backward' Nonclassical Particle Transport Theories," these Proceedings.